The role of the thermohaline circulation in abrupt climate change

Peter U. Clark*, Nicklas G. Pisias†, Thomas F. Stocker‡ & Andrew J. Weaver§

* *Department of Geosciences, Oregon State University, Corvallis, Oregon 97331, USA*
† *College of Oceanic and Atmospheric Sciences, Oregon State University, Corvallis, Oregon 97331, USA*
‡ *Climate and Environmental Physics, University of Bern, Physics Institute, Sidlerstrasse 5, 3012 Bern, Switzerland*
§ *School of Earth and Ocean Sciences, University of Victoria, PO Box 3055, Victoria, British Columbia V8W 3P6, Canada*

The possibility of a reduced Atlantic thermohaline circulation in response to increases in greenhouse-gas concentrations has been demonstrated in a number of simulations with general circulation models of the coupled ocean–atmosphere system. But it remains difficult to assess the likelihood of future changes in the thermohaline circulation, mainly owing to poorly constrained model parameterizations and uncertainties in the response of the climate system to greenhouse warming. Analyses of past abrupt climate changes help to solve these problems. Data and models both suggest that abrupt climate change during the last glaciation originated through changes in the Atlantic thermohaline circulation in response to small changes in the hydrological cycle. Atmospheric and oceanic responses to these changes were then transmitted globally through a number of feedbacks. The palaeoclimate data and the model results also indicate that the stability of the thermohaline circulation depends on the mean climate state.

The ocean affects climate through its high heat capacity relative to the surrounding land, thereby moderating daily, seasonal and interannual temperature fluctuations, and through its ability to transport heat from one location to another. In the North Atlantic, differential solar heating between high and low latitudes tends to accelerate surface waters polewards whereas freshwater input to high latitudes together with low-latitude evaporation tend to brake this flow. Today, the former thermal forcing dominates the latter haline (freshwater) forcing and the meridional overturning in the Atlantic drives surface waters northward, while deep water that forms in the Nordic Seas flows southward as North Atlantic Deep Water (NADW). This thermohaline circulation (THC) is responsible for much of the total oceanic poleward heat transport in the Atlantic, peaking at about 1.2 ± 0.3 PW (1 PW equals 10^{15} watts) at 24° N (ref. 1).

No such deep overturning occurs in the North Pacific, where surface waters are too fresh to sink[2]. The lack of a meridional land barrier in the Southern Ocean precludes the existence of strong east–west pressure gradients needed to balance a southward geostrophic surface flow, so that poleward heat transport associated with the THC is small there. Deep-water formation in the Southern Ocean occurs along the Antarctic continental shelf in the Weddell and Ross Seas either through intense evaporation or, more typically, through brine rejection that produces dense water that sinks down and along the slope[3]. In addition, supercooled water may be formed at the base of the thick floating ice shelves during freezing or melting and this dense water may in turn flow downslope[4].

The idea that the Atlantic THC may have many speeds is now a century old[2], but not until the 1960s did a quantitative, albeit idealized, framework emerge to explain the physics behind the potential existence of these multiple equilibria[5]. Subsequently, ocean[6] and coupled atmosphere–ocean general circulation models (GCMs) (ref. 7) were shown to support multiple equilibria. Such studies have revealed that multiple equilibria exist because the atmosphere responds to anomalies of sea surface temperature, but not salinity[8]. They have further shown that transitions between different states are often abrupt and can be induced through small perturbations to the hydrological cycle.

The concept of multiple equilibria of the THC and the transitions between these states is now commonly invoked as a mechanism to explain the abrupt climate changes that were characteristic of the last glaciation[9,10]. Here we refer to an abrupt change as a persistent transition of climate (over subcontinental scale) that occurs on the timescale of decades. Although understanding the mechanisms behind abrupt climate transitions in the past is interesting in its own right, there is a pressing need to gain insight into the likelihood of their future occurrence[11,12]. Most, but not all, coupled GCM projections of the twenty-first century climate show a reduction in the strength of the Atlantic overturning circulation with increasing concentrations of greenhouse gases[13]—if the warming is strong enough and sustained long enough, a complete collapse cannot be excluded[14,15]. The successful simulation of past abrupt events that are found in the palaeoclimate record is the only test of model fidelity in estimating the possibility of large ocean–atmosphere reorganizations when projecting future climate change.

Past changes in the thermohaline circulation

Considerable progress has been made in linking past abrupt changes in North Atlantic surface-ocean and atmospheric temperature with changes in deep ocean circulation, confirming the important role that major reorganizations of the Atlantic THC have played in abrupt climate change. Although a continuum of possible modes of NADW formation may exist[16], palaeoceanographic records suggest that the largest changes in North Atlantic climate were associated with transitions among three possible modes: a modern mode, a glacial mode, and a Heinrich mode[9]. The modern mode is characterized by the formation of deep water in the Nordic Seas and its subsequent flow over the Greenland–Scotland ridge[17]. The newly formed NADW flows into the Labrador Sea where it entrains recirculating, relatively cold and fresh Labrador Sea intermediate waters[17] that are largely confined to the subpolar gyre of the North Atlantic[18] before progressing southward. During the glacial mode, NADW probably formed through open-ocean convection in the subpolar North Atlantic, sinking to depths of less than 2,500 m (ref. 19). Buoyancy loss by brine rejection under sea ice in the Nordic Seas may have provided an additional source of glacial-mode NADW[20]. Finally, during the Heinrich mode, Antarctic-derived waters filled the North Atlantic basin to depths as shallow as 1,000 m (ref. 21).

Changes in the location, depth and volume of newly formed NADW associated with mode shifts are now relatively well constrained, but the magnitude of related changes in the rate of the overturning circulation and deep ocean ventilation remains controversial[22,23]. In this regard, atmospheric radiocarbon (expressed as $\Delta^{14}C_{atm}$, the per mil deviation from a ^{14}C standard after correction for radioactive decay and fractionation) offers great promise for identifying past changes in the globally integrated THC. $\Delta^{14}C_{atm}$ is a function of the production rate of ^{14}C in the upper atmosphere and the sizes of and exchange rates between the major carbon reservoirs. Considerable work yet remains before production-rate effects are quantified so as to yield a residual $\Delta^{14}C_{atm}$ signal that uniquely reflects changes in ocean ventilation back to 22.0 kyr before present (BP), or the period in which existing records show coherent changes in $\Delta^{14}C_{atm}$ (Fig. 1a). As a first approximation, we account for the long-term decrease in ^{14}C production rate that resulted primarily from a gradual increase in the geomagnetic field intensity over the last 22 kyr (ref. 24), isolating changes in $\Delta^{14}C_{atm}$ that, on shorter timescales ($\leq 10^3$ yr), are largely due to changes in cosmic radiation or ocean ventilation.

Polar ice core records of the cosmogenic radionuclide ^{10}Be can be used to estimate past changes in cosmic radiation because ^{10}Be is rapidly (1–2 yr) removed from the atmosphere to the ice surface by precipitation. On this basis, the ^{10}Be record from the GISP2 ice core[25] suggests that changes in cosmogenic production rates are an unlikely cause of first-order changes in $\Delta^{14}C_{atm}$ between 15.0 and 22.0 kyr (Fig. 1b). Between 11.5 and 15.0 kyr BP, the ^{10}Be signal in the GISP2 ice core is more strongly influenced by climate, but a detailed analysis suggests that a geomagnetic influence may have been important in explaining the decrease in $\Delta^{14}C_{atm}$ during the Younger Dryas cold event[26,27] (Fig. 1a). The two large increases in ^{10}Be flux at 10.1 and 11.1 kyr BP, which may reflect solar variability[26], correspond to two increases in $\Delta^{14}C_{atm}$ of about 30‰. (The small age offsets indicate that the GISP2 timescale is too old in this interval by about 60 years[26].) In contrast, the fluctuations in $\Delta^{14}C_{atm}$ before 14.6 kyr BP with amplitudes of over 80‰ do not have corresponding fluctuations in ^{10}Be flux, and thus probably reflect changes in the THC, although a geomagnetic influence cannot yet be ruled out for explaining some of the signal.

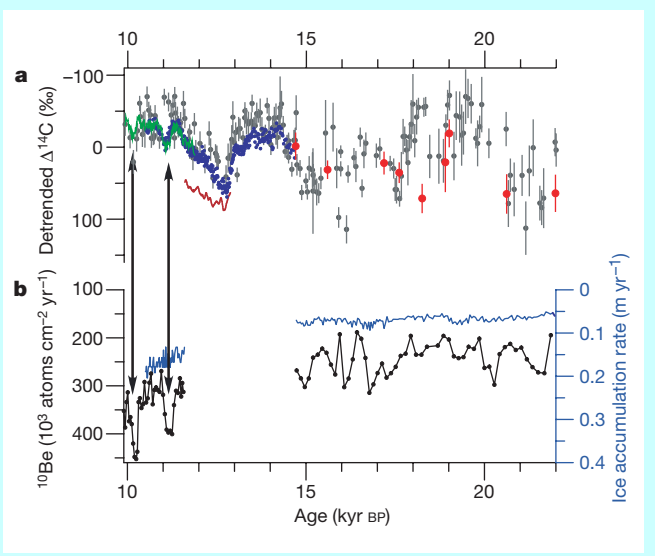

Figure 1 Comparison of record of linearly detrended $\Delta^{14}C_{atm}$ to ^{10}Be flux data from the GISP2 ice core. **a**, Linearly detrended records of $\Delta^{14}C_{atm}$ used to infer changes in the global thermohaline circulation between 9.9 and 22.0 kyr BP. Records include tree rings (solid green line)[72], varves from the Cariaco basin (blue circles)[33], varves from Lake Suigetsu, Japan (grey circles with error bars)[73], and U/Th-dated corals (red circles with error bars)[74]. The thin red line is an estimate of production-rate decrease in $\Delta^{14}C_{atm}$ between 11.5 and 12.9 kyr BP (from ref. 26 with age model modified to be on GISP2 timescale); vertical scale is offset by 80‰. We linearly detrended the combined $\Delta^{14}C_{atm}$ records for the interval 5 to 25 kyr in order to account for the long-term decrease in ^{14}C production rate that resulted primarily from a nearly linear increase in the geomagnetic field intensity over this time[24]. Short-term variations in the geomagnetic field intensity may also contribute, but existing geomagnetic records showing variability during this interval are not coherent. **b**, Records of ^{10}Be flux (filled circles) and ice accumulation rate (blue line) from GISP2 ice core. ^{10}Be flux is the product of the ^{10}Be concentration[25] and the ice accumulation rate[75] averaged over the sample interval of the ^{10}Be measurements. We do not show the accumulation rate and ^{10}Be flux records from 14.6 to 11.5 kyr BP because the ^{10}Be flux variations in this interval are dominated by the large variations in snow accumulation rate, thus obscuring production-rate controls on ^{10}Be during this time. Accumulation-rate variability was small before 14.6 kyr BP, thus indicating that there is little potential influence of changes in snowfall rate on ^{10}Be flux.

NADW is presently the major source of ^{14}C to the deep sea[28], and changes in the strength of this water mass (and its preformed properties) probably dominate the variations in $\Delta^{14}C_{atm}$ associated with the global carbon cycle over the last 22.0 kyr. These changes can be modulated by changes in the THC elsewhere, but surface waters in the Southern Ocean and North Pacific are now old[28], and may have been significantly older during glacial periods[29], suggesting that any increase in formation of deep or intermediate waters in these regions will have a lesser impact on the $\Delta^{14}C_{atm}$ budget than changes in NADW.

The hypothesis that changes in $\Delta^{14}C_{atm}$ largely reflect variations in the Atlantic THC is supported by the relation between first-order changes in $\Delta^{14}C_{atm}$ and in proxies that record changes in the volume of NADW and North Atlantic climate (Fig. 2). High $\Delta^{14}C_{atm}$ during the Last Glacial Maximum (LGM) (Fig. 2c) is associated with the glacial mode of NADW[19] and cold North Atlantic atmospheric[30] (Fig. 2d) and sea surface[31] (Fig. 2e) temperatures. The subsequent decrease in $\Delta^{14}C_{atm}$ to essentially interglacial levels was associated with warming in the North Atlantic region, while a subsequent long-term increase between 19.0 kyr BP to 14.7 kyr BP coincides with the Oldest Dryas cooling, during which Heinrich event 1 (H1) occurred (~17.5 kyr BP) (Fig. 2b). During H1, $\Delta^{14}C_{atm}$ rapidly increased to levels similar to the LGM (Fig. 2c), whereas the volume of NADW during the Heinrich mode (as inferred from geochemical proxies) was <50% of that during the LGM[21]. Relative to the glacial mode, these relations suggest that the Heinrich mode reflects some combination of further shallowing of NADW to intermediate depths while maintaining similar rates of overturning, and a compensatory increase in deep-water formation elsewhere.

A large decrease in $\Delta^{14}C_{atm}$ to interglacial levels coincides with the onset of the Bølling–Allerød warm interval at around 14.7 kyr BP; the abrupt warming recorded in the GISP2 ice core[32] (Fig. 2d) appears to be a nonlinear response to the more gradual increase in the THC (Fig. 2c). A subsequent increase in $\Delta^{14}C_{atm}$ began precisely at the onset of the Younger Dryas cold interval at 13.0 kyr BP (Fig. 2c)[33]. The decrease in $\Delta^{14}C_{atm}$ during the remainder of the Younger Dryas may be the result of an increase in the production rate of ^{14}C (refs 26, 27) (Fig. 1a), suggesting that the THC remained weakened until the end of the Younger Dryas at 11.5 kyr BP when it abruptly switched back to the modern mode[27].

Mechanisms of past abrupt climate changes

The freshwater budget in the North Atlantic is one of the major components that governs the strength of the Atlantic THC, and dynamical ocean models show that the THC is sensitive to freshwater perturbations on order of 0.1 Sv ($1\,Sv = 10^6\,m^3\,s^{-1}$) (refs 34–36). A clear goal for understanding past changes in the THC, therefore, is to identify the mechanisms that influenced the North Atlantic freshwater budget. Reconstructions of changes in the freshwater flux from ice sheets around the North Atlantic reveal good agreement with past changes in the THC and North Atlantic climate (Fig. 2a–e), identifying these processes as being important

in causing abrupt climate change[37,38]. Paradoxically, although the THC in current models responds to freshwater forcings without delay, the largest deglacial meltwater event on record, referred to as meltwater pulse 1A (MWP-1A), occurs more than 1,000 years before the next significant change in the THC associated with the Younger Dryas cold interval[39]. This paradox may be resolved, however, if MWP-1A originated largely from the Antarctic Ice Sheet[40], where its impact on the Atlantic THC would be substantially reduced.

Millennial-scale (10^3 yr) changes in the Atlantic THC that involved transitions from modern to glacial modes of NADW are manifested as dramatic fluctuations of North Atlantic climate referred to as Dansgaard–Oeschger (D–O) events, each having a characteristic pattern of abrupt (years to decades) warming

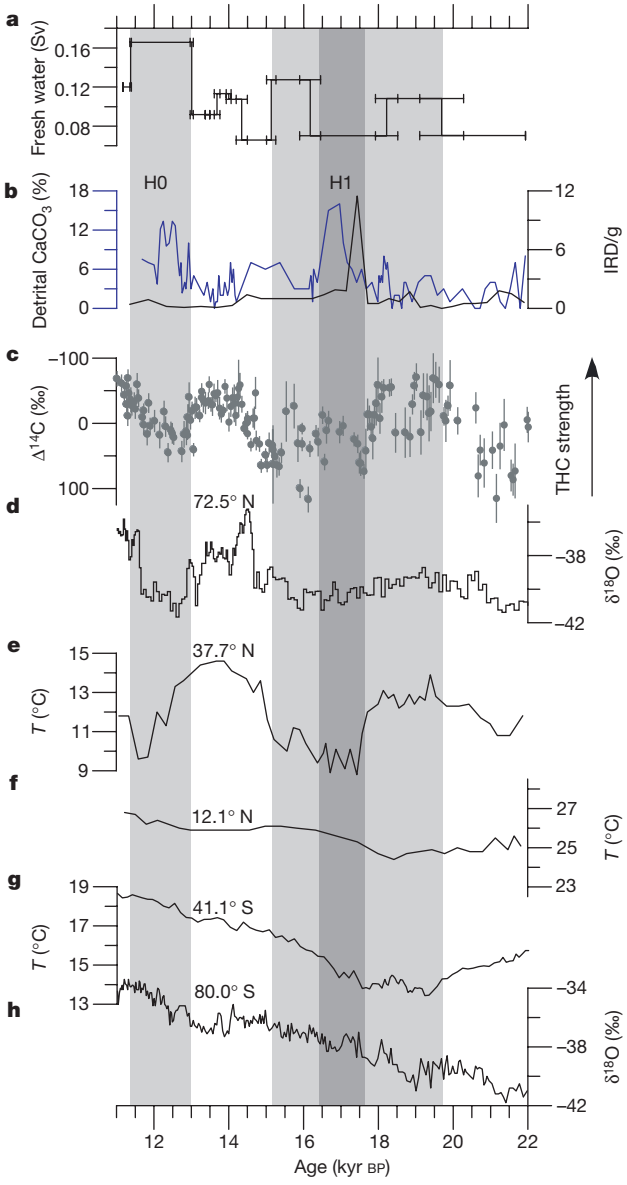

Figure 2 Comparison of reconstructed forcings and responses in the Atlantic basin during the last deglaciation (11–22 kyr BP). Time series of changes in freshwater forcing (**a**, **b**) and response of the THC as inferred by first-order changes in $\Delta^{14}C_{atm}$ (**c**). Panels **d**–**h** show atmospheric and sea surface temperature changes during the last deglaciation along a north–south transect of the Atlantic basin (72.5° N to 80° S), illustrating the operation of the bipolar seesaw in response to large changes in the Atlantic THC. **a**, Changes in freshwater runoff from North America through the Hudson and St Lawrence Rivers[38]. Two vertical light-grey bars identify intervals of enhanced freshwater flux to the North Atlantic from these sources as well as from icebergs inferred from records (not shown) of total ice-rafted debris (IRD)[37]. **b**, Changes in the amount of IRD containing detrital carbonate lithologies, with large increases identifying times of Heinrich events H1 (identified by darker-grey vertical bar) and H0. The IRD records are from North Atlantic cores VM23-081 (blue curve)[37] and SU8118 (black curve)[31]. **c**, Detrended record of $\Delta^{14}C_{atm}$ from Lake Suigetsu, Japan[73], with first-order changes indicating changes in the meridional overturning of the Atlantic THC (see text); a stronger THC is indicated by more negative values of $\Delta^{14}C_{atm}$. **d**, The GISP2 ice-core oxygen-isotope record[76,77]. Results of calibrating the isotopic palaeothermometer by various methods show a temperature depression of 20 °C at the Last Glacial Maximum ~21.0 kyr BP (ref. 30), a warming of 10 °C at the onset of the Bølling at ~14.6 kyr BP (ref. 32), and a warming of 15 °C at the end of the Younger Dryas ~11.5 kyr BP (ref. 41). **e**, Record of sea surface temperatures (SSTs) derived from alkenones measured in North Atlantic core SU8118 (ref. 31). **f**, Record of SSTs derived from alkenones measured in tropical North Atlantic core M35003-4 (ref. 78). **g**, Record of SSTs derived from alkenones measured in South Atlantic core TN057-21-PC2 (ref. 79). The timescale for this record is provisional (J. Sachs, personal communication). **h**, The Byrd ice-core oxygen-isotope record[50].

followed by gradual (centuries) cooling. The largest changes (>15 °C over Greenland)[41] occurred during times of intermediate global ice volume, CO_2, or insolation[42]. In Greenland ice core records, abrupt warmings exhibit a preferred waiting time of 1,500 ± 500 yr (ref. 43). This spacing is similar to a 1,000–2,000-yr climate cycle identified from marine records during interglacial as well as glacial periods, leading some to speculate that D–O events may be amplified expressions of an ongoing persistent and stable climate cycle[37,43]. However, this timescale of variability does not constrain one mechanism over another. Several mechanisms may have operated jointly, and the relative contribution of potential mechanisms probably changed in response to the large-scale changes in global boundary conditions that accompanied the last deglaciation.

Atmospheric transmission of the D–O signal beyond the North Atlantic region is suggested by high-resolution climate records that display the same structure of change that, within dating uncertainties, is synchronous with the North Atlantic signal. It is also suggested by simulations using atmospheric GCMs[44], although these models have yet to include all potential feedbacks that may be important in transmitting the signal to regions far from the North Atlantic. Greenland ice-core records of methane and $\delta^{18}O$ strongly support the hypothesis of North Atlantic forcing in showing a nearly instantaneous response of the tropical water balance to changes in high-latitude temperature[32,41]. Palaeoclimate records identify additional atmospheric responses to North Atlantic climate that would potentially further amplify and transmit the D–O signal. These include changes in (1) the strength of trade winds and associated oceanic upwelling[45], (2) the position of the Intertropical Convergence Zone, with attendant effects on water vapour transport for the Atlantic to the Pacific basin[46], (3) the strength of the Asian monsoon[47], (4) sea surface temperatures of the Pacific warm pool[48] and (5) ventilation of the North Pacific[49].

A large reduction in the THC during the Heinrich mode (Fig. 2c) causes additional cooling in the North Atlantic[31] (Fig. 2e), while contemporaneous warming observed in some regions of the Southern Hemisphere[9,50] indicates that the large reduction in NADW formation decreased meridional heat transport from the South Atlantic (Fig. 2f–h). A similar 'bipolar seesaw' effect may hold for the Younger Dryas event[51] (Fig. 2), but the absence of a comparable thermally antiphased southern signal associated with many of the older D–O events[50] suggests that any changes in oceanic heat transport accompanying the changes from modern to glacial circulation modes were either too small or too short to be clearly registered in existing climate records.

We thus expect to see two mechanisms of variability in climate related to changes in the THC: one associated with atmospheric transmission and one associated with an oceanic seesaw, although these are not independent as an oceanic change necessarily implies an atmospheric response and vice versa. We use empirical orthogonal function (EOF) analysis to provide an objective characterization of these modes of climate variability during the last deglaciation by reducing 18 well-dated time series of climate change (Fig. 3) into spatially coherent, orthogonal eigenvectors. Our analysis indicates that the last deglaciation was dominated by two climate responses. The first EOF (68% of variance) captures the global warming from glacial to interglacial conditions that evolved over a timescale of about 10 kyr. Included in this EOF is the interruption of the warming trend by the Younger Dryas. The second EOF (15% of the variance) quantifies the spatial and temporal expression of millennial changes centred at 16 and 12 kyr BP (Fig. 3a). The spatial pattern of this EOF, with negative scores over Antarctica (except Taylor Dome) and in the South Atlantic and positive scores at all other sites (Fig. 4b), is consistent with an atmospheric transmission of the North Atlantic signal except for those areas in the Southern Hemisphere where operation of the seesaw during the last deglaciation produced an antiphased response as predicted by a large change in the THC[52–54]. We find that a similar spatial pattern holds for the interval between 26 and 50 kyr BP, indicating that the seesaw operated during this time as well[50].

Modelling abrupt climate change

Modelling abrupt climate change faces several challenges: (1) a disparity in timescales between transient states (lasting many centuries) and mode changes (occurring in a few years to decades); (2) a compromise in model complexity due to long integrations and sufficient model resolution to capture abruptness; and (3) uncertainties in initial conditions due to patchy coverage as well as calibration problems in palaeoclimatic proxy data. Although at present there exists no self-consistent model that simulates, without prescribed forcing, changes that resemble the palaeoclimatic record, important progress has been made.

Abrupt change manifests itself in two different ways in climate models: an abrupt transition across a threshold to a new equilibrium state, or a response to a fast forcing. Although multiple equilibria are not necessary for abrupt change[35], the palaeoclimatic records suggest that the ocean–atmosphere system may have preferred modes of operation, that is, the system operates like a 'flip-flop' mechanism[55]. This implies the existence of hysteresis of the THC[16,34,56], which appears to be common in coupled climate models. However, the shape and structure of the hysteresis loop strongly depends on model parameters and therefore is still a tunable feature[57] so that the exact location of thresholds cannot yet be determined with current models. Nevertheless, it is clear that thresholds and hence the stability properties of the THC depend fundamentally on the mean climate state[8,58].

A number of ocean and coupled atmosphere–ocean models have found the existence of three distinct modes of the conveyor that are qualitatively the same as the modern, glacial and Heinrich modes identified by palaeoclimate data[16,59,60]. These and other models have also revealed that transitions can be triggered by changes in the freshwater balance of the North Atlantic and changes in modes are associated with changes in the heat budget of the Atlantic basin. For large reductions in NADW formation, this leads to the same 'seesaw effect' seen in the data[34,52,53] (Figs 2, 4).

Recent modelling ideas postulate an atmosphere–ocean system during the last glaciation that was extremely close to a threshold, thus requiring very weak freshwater forcing to trigger abrupt changes of the THC[16,60]. Whether the sequence of abrupt events originates from unknown periodic forcing[43,60] or instabilities and feedbacks associated with circum-Atlantic ice sheets[16,38] remains an open question. Furthermore, qualitative consistence with the palaeoclimatic records remains very sensitive to parameter choices in these models. The basic question about the origin of abrupt change is therefore not solved. However, all model simulations until now point towards the key role of the freshwater balance in the Atlantic Ocean. More realistic models and improved reconstructions of the various components of the hydrological cycle (precipitation, run-off, iceberg discharge, sea ice) are urgently needed.

Progress towards a mechanistic understanding of abrupt climate change can be expected from more complete models. These are coupled models with higher resolution, models that no longer require flux adjustments, and models that include biogeochemical cycles. The latter will enable a direct and quantitative comparison with palaeoclimatic data (for example, the stable isotopes of water and carbon), and significantly facilitate model-based hypothesis testing. The tracer $\Delta^{14}C_{atm}$ affords additional constraints and helps to estimate how much of the observed changes (Fig. 1a) can be associated with changes in the THC[27]. Results based on simplified ocean models show that a shutdown of the Atlantic THC produces a significant increase in $\Delta^{14}C_{atm}$ but the amplitudes are only about half of those observed[27]. Further model simulations are needed

to fully explore the dependence of $\Delta^{14}C_{atm}$ changes on model parameters.

Tropical Pacific variability represents the dominant mode of modern climate variability with its effects felt across the globe. Although a basic understanding of the physics of ENSO has been achieved, it is still not clear how ENSO responds in colder and warmer mean climates. For example, some models suggest that tropical Pacific variability will remain similar to the present, whereas others suggest stronger and more frequent warm events could be in store in a warmer future climate. Nevertheless, it is apparent that Atlantic-to-Pacific moisture transport is sensitive to the phase of ENSO[61], so that a persistent trend towards an enhanced frequency of warm events[62] could lead to an increase in net export of moisture from the Atlantic across the Isthmus of Panama, thereby possibly affecting the THC.

Discussion

Publication of the results from the first ice core from Summit, Greenland, detailing abrupt climate change during the last glaciation[63] motivated an intensive investigation for evidence of similar climate instability occurring elsewhere on the globe and its causes. The resulting palaeoclimate records clearly reveal the global extent of millennial-scale climate variability, with varying responses that are consistent with atmospheric and oceanic changes associated

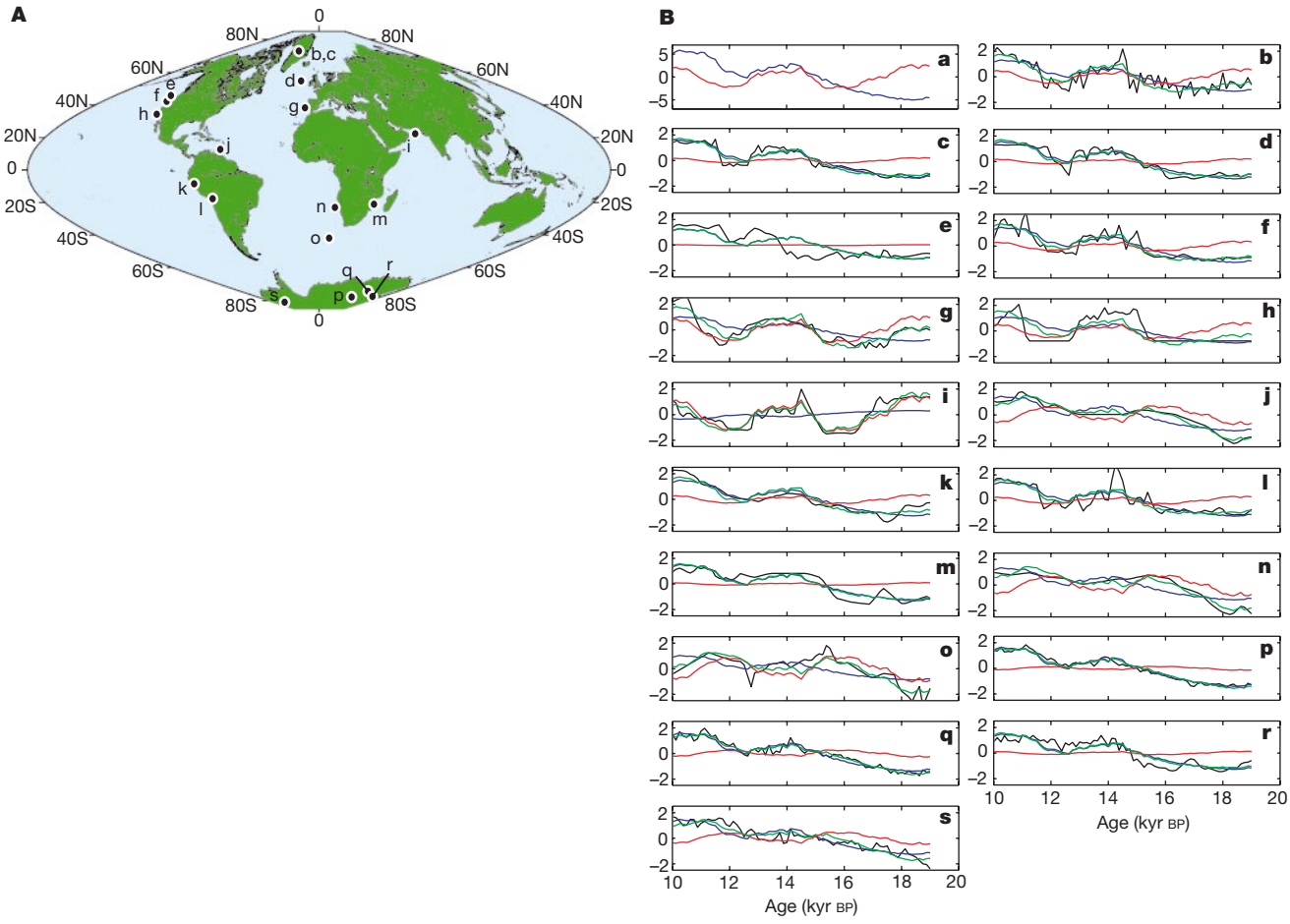

Figure 3 Time-history of the first two empirical orthogonal functions (EOFs) determined from 18 time series. **A**, Data sampling locations. **B**, Time series. These data sets provide time series of climate change with temporal sampling resolution of about 250 years or less. All time series were interpolated to a constant sampling interval of 125 years. Numerical experiments demonstrate that the results presented here are insensitive to factor-of-2 changes in the selected constant sampling interval. All data sets were then transformed to mean zero and standard deviation of one. We note that where the second EOF is negative, time series are characterized by early warming but a weaker Younger Dryas; where the second EOF is positive, the Younger Dryas tends to be a more significant event. We emphasize that the pattern of the second EOF depends strongly on the quality of the timescale and the precision of the synchronization between these palaeoclimatic records (for example refs 80, 81). **a**, The time series for the first two EOFs, where the blue line is the first EOF and the red line is second EOF. The first EOF accounts for 68% of the data variance while the second EOF accounts for 15%. **b**–**s**, Plots of the original time series and the results of the EOF analysis. The normalized time series from each location (black line), the weighted EOFs using the weights from **a** (blue line is first EOF, red line is second EOF), and the sum of the first two EOFs (green line). **b**, Oxygen-isotope record from the GISP2 ice core[76,77]. **c**, Methane record from the GISP2 ice core[50]. **d**, Percentages of *Neogloboquadrina pachyderma* (s.) from North Atlantic core VM23-81 (ref. 37). **e**, Relative abundance of a radiolarian assemblage identified in northeastern Pacific core EW9504-17PC (ref. 82). **f**, Percentages of *N. pachyderma* (s.) from ODP Site 1019 in the northeastern Pacific[83]. **g**, Alkenone-derived sea surface temperatures from the subtropical northeast Atlantic[31]. **h**, Changes in the bioturbation index from ODP Site 893 in the Santa Barbara basin[49]. **i**, Total organic carbon from Arabian Sea sediments[47]. **j**, Alkenone-derived sea surface temperatures from the tropical North Atlantic[78]. **k**, Oxygen-isotope record from the Huascaran ice core, Peru[84]. **l**, Oxygen isotope record from the Sajama ice core, Bolivia[85]. **m**, Alkenone-derived sea surface temperatures from the tropical Indian Ocean[86]. **n**, Percentages of *N. pachyderma* (s.) from the South Atlantic[87]. **o**, Residual oxygen-isotope record measured on planktonic foraminifera for the South Atlantic[88]. **p**, The Vostok ice-core deuterium record[89]. **q**, Deuterium record from the Dome C ice core[90]. **r**, Oxygen-isotope record from the Taylor Dome ice core[80]. **s**, Oxygen-isotope record from the Byrd ice core[50].

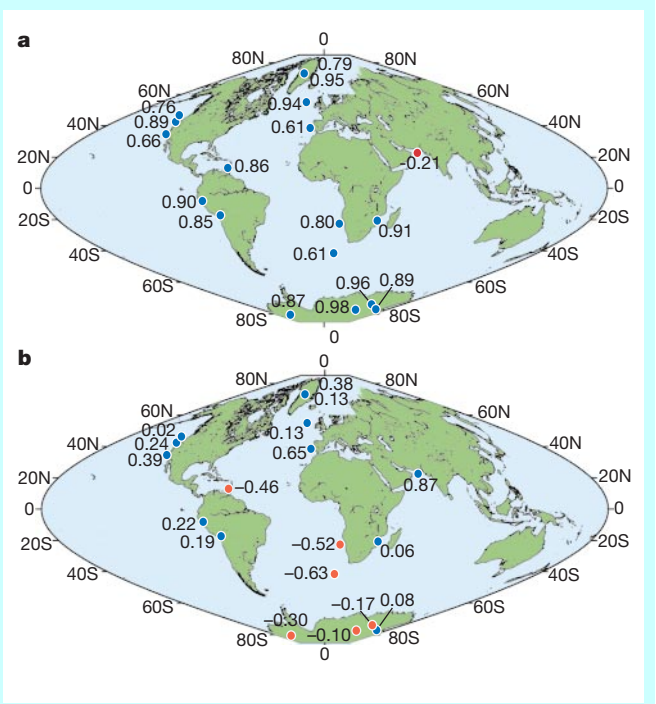

Figure 4 The spatial pattern of the first two empirical orthogonal functions extracted from the data set (see Fig. 3a). Numbers shown are loadings of the first two EOFs for 18 deglacial time series. Loadings indicate the importance of each EOF in explaining the variations in each time series. To reconstruct the normalized (mean zero and standard deviation of one) time series at any one location, we take the loadings shown in Fig. 3a, multiply them by the time series of the EOFs and add them together. The two loadings next to the Greenland site correspond to the GISP2 oxygen isotope (upper) and methane (lower) records. **a**, First EOF; **b**, second EOF.

with changes in the Atlantic THC (Figs 3, 4). Moreover, the relation between times of increased freshwater flux to the North Atlantic and corresponding decreases in the THC (Fig. 2) supports modelling results showing that the THC was sensitive to small changes in the hydrological cycle (order of 0.1 Sv) during the last glaciation[35,36,60].

With respect to cause and effect, however, our understanding of abrupt climate change remains incomplete. Insofar as the palaeoclimate record provides the fundamental basis for evaluating the ability of models to correctly simulate behaviour of the THC, additional information is needed to address these issues. In particular, several areas that require immediate attention include: (1) an increase in the distribution of sites in the Pacific and Southern Oceans; (2) development of new tools to synchronize palaeoclimatic records and constrain phasing relations; (3) improvements in calibrating the climate signal from proxy records; and (4) further analysis of the $\Delta^{14}C_{atm}$ record for the last 50 kyr BP.

A variety of simulations from coupled models of varying complexities are beginning to simulate the temporal evolution and global signature of millennial-scale change revealed by the palaeoclimate record, and provide important insights into the mechanisms of change. In particular, palaeoclimate records and modelling experiments are providing a framework for the possible magnitude of future warming and the response of the interconnected Earth system to such a warming. Moreover, coupled GCM experiments incorporating geologic data (for example, continental runoff history)[36,64] provide new constraints on the mechanisms of abrupt climate change and will lead to model improvements that are essential for achieving the ability to simulate future climate. Nevertheless, modelling past abrupt climate change remains one of the greatest challenges for palaeoclimate modellers. Further progress will probably be realized as fully interactive and non-flux adjusted coupled Earth system models are developed that treat the full range of climate feedbacks[16].

Some modelling experiments find that during the next few centuries, the THC moves to an 'off' state in response to increasing greenhouse gases[14,15,65]. A reduction of the meridional heat transport into the circum-Atlantic region would partially compensate the warming due to increasing greenhouse gases, although such a change could have serious climatic consequences for the climate in the circum-Atlantic region through modifying long-established regional air–sea temperature contrasts, seasonal variations in the direction and strength of wind patterns[66] and the location of convective areas[67]. The implication of such changes on regional climate remains largely unexplored. Reorganizations in the THC would also change the distribution of water masses and hence the density in the world ocean. A warmer and more stratified North Atlantic would also take up less anthropogenic CO_2 (ref. 68). On the other hand, other experiments suggest little or no reduction of the THC to the same greenhouse gas forcing[13]. This indicates the possible dominance of negative feedback mechanisms such as changes in the amplitude and frequency of ENSO[69], or modifications of atmospheric variability patterns in the Northern Hemisphere[70].

The fate of the THC in the coming century largely depends on the response of air–sea heat and freshwater fluxes to the increased load of greenhouse gases. Uncertainties in modelled responses are particularly large for the latter[13]. Moreover, the threshold for the occurrence of an abrupt change in a particular climate model depends on poorly constrained parameterizations of sub-grid-scale ocean mixing[57]. Because a complete THC shutdown is a threshold phenomenon, the assessment of the likelihood of such an event must involve ensemble model simulations[71], as well as continued efforts to simulate past abrupt climate changes that so remarkably affected the global climate system. □

1. Ganachaud, A. & Wunsch, C. Improved estimates of global ocean circulation, heat transport and mixing from hydrographic data. *Nature* **408,** 453–457 (2000).
2. Weaver, A. J., Bitz, C. M., Fanning, A. F. & Holland, M. M. Thermohaline circulation: High latitude phenomena and the difference between the Pacific and Atlantic. *Annu. Rev. Earth Planet. Sci.* **27,** 231–285 (1999).
3. Killworth, P. D. Deep convection in the world ocean. *Rev. Geophys. Space Phys.* **21,** 1–26 (1983).
4. Grumbine, R. W. A model of the formation of high-salinity shelf water on polar continental shelves. *J. Geophys. Res.* **96,** 22049–22062 (1991).
5. Stommel, H. Thermohaline convection with two stable regimes of flow. *Tellus* **13,** 224–230 (1961).
6. Bryan, F. High-latitude salinity effects and interhemispheric thermohaline circulations. *Nature* **323,** 301–304 (1986).
7. Manabe, S. & Stouffer, R. J. Two stable equilibria of a coupled ocean-atmosphere model. *J. Clim.* **1,** 841–866 (1988).
8. Weaver, A. J. in *Natural Climate Variability on Decade-to-Century Time Scales* (eds Martinson, D. G. *et al.*) 365–381 (National Research Council, National Academy Press, Washington DC, 1995).
9. Alley, R. B. & Clark, P. U. The glaciation of the northern hemisphere: a global perspective. *Annu. Rev. Earth Planet. Sci.* **27,** 149–182 (1999).
10. Stocker, T. F. Past and future reorganization in the climate system. *Quat. Sci. Rev.* **19,** 301–319 (2000).
11. Broecker, W. S. Thermohaline circulation, the Achilles heel of our climate system: Will man-made CO_2 upset the current balance? *Science* **278,** 1582–1588 (1997).
12. Alley, R. B. *et al. Abrupt Climate Change: Inevitable Surprises* (National Research Council, National Academy Press, Washington DC, in the press).
13. Cubasch, U. *et al.* in *Climate Change 2001—The Scientific Basis: Contribution of Working Group I to the Third Assessment Report of the Intergovernmental Panel on Climate Change* (eds Houghton, J. T. *et al.*) 525–582 (Cambridge Univ. Press, Cambridge, 2001).
14. Manabe, S. & Stouffer, R. J. Century-scale effects of increased atmospheric CO_2 on the ocean-atmosphere system. *Nature* **364,** 215–218 (1993).
15. Stocker, T. F. & Schmittner, A. Influence of CO_2 emission rates on the stability of the thermohaline circulation. *Nature* **388,** 862–865 (1997).
16. Schmittner, A., Yoshimori, M. & Weaver, A. J. Instability of glacial climate in an earth system model. *Science* (in the press).
17. Dickson, R. R. & Brown, J. The production of North Atlantic deep water: Sources, sinks and pathways. *J. Geophys. Res.* **99,** 12319–12341 (1994).
18. McCartney, M. S. Recirculating components to the deep boundary current of the northern North Atlantic. *Prog. Oceanogr.* **29,** 283–383 (1992).
19. Labeyrie, L. *et al.* Changes in vertical structure of the North Atlantic Ocean between glacial and modern times. *Quat. Sci. Rev.* **11,** 401–413 (1992).
20. Vidal, L., Labeyrie, L. & van Weering, T. C. E. Benthic $\delta^{18}O$ records in the North Atlantic over the last glacial period (60–10 kyr): Evidence for brine formation. *Paleoceanography* **13,** 245–251 (1998).
21. Sarnthein, M. *et al.* Changes in east Atlantic deepwater circulation over the last 30,000 years: Eight time slice reconstructions. *Paleoceanography* **9,** 209–267 (1994).

22. Yu, E. F., Francois, R. & Bacon, M. P. Similar rates of modern and last-glacial ocean thermohaline circulation inferred from radiochemical data. *Nature* **379,** 689–694 (1996).
23. Rutberg, R. L., Hemming, S. R. & Goldstein, S. L. Reduced North Atlantic Deep Water flux to the glacial Southern Ocean inferred from neodymium isotope ratios. *Nature* **405,** 935–938 (2000).
24. Frank, M. Comparison of cosmogenic radionuclide production and geomagnetic field intensity over the last 200,000 years. *Phil. Trans. R. Soc. Lond. A* **358,** 1089–1107 (2000).
25. Finkel, R. C. & Nishiizumi, K. Beryllium 10 concentrations in the Greenland Ice Sheet Project 2 ice core from 3–40 ka. *J. Geophys. Res.* **102,** 26699–26706 (1997).
26. Muscheler, R., Beer, J., Wagner, G. & Finkel, R. C. Changes in deep-water formation during the Younger Dryas event inferred from ^{10}Be and ^{14}C records. *Nature* **408,** 567–570 (2000).
27. Marchal, O., Stocker, T. F. & Muscheler, R. Atmospheric radiocarbon during the Younger Dryas: production, ventilation, or both? *Earth Planet Sci. Lett.* **185,** 383–395 (2001).
28. Broecker, W. S., Mix, A., Andree, M. & Oeschger, H. Radiocarbon measurements on coexisting benthic and planktic foraminifera shells: potential for reconstructing ocean ventilation times over the past 20000 years. *Nucl. Instrum. Methods Phys. Res.* **B5,** 331–339 (1984).
29. Sikes, E. L., Samson, C. R., Guilderson, T. P. & Howard, W. R. Old radiocarbon ages in the southwest Pacific Ocean during the last glacial period and deglaciation. *Nature* **405,** 555–559 (2000).
30. Cuffey, K. M. *et al.* Large Arctic temperature change at the Wisconsin-Holocene glacial transition. *Science* **270,** 455–458 (1995).
31. Bard, E., Rostek, F., Turon, J.-L. & Gendreau, S. Hydrological impact of Heinrich events in the subtropical northeast Atlantic. *Science* **289,** 1321–1324 (1999).
32. Severinghaus, J. P. & Brook, E. J. Abrupt climate change at the end of the last glacial period inferred from trapped air in polar ice. *Science* **286,** 930–934 (1999).
33. Hughen, K. A., Southon, J. R., Lehman, S. J. & Overpeck, J. T. Synchronous radiocarbon and climate shifts during the last deglaciation. *Science* **290,** 1951–1954 (2000).
34. Stocker, T. F. & Wright, D. G. Rapid transitions of the ocean's deep circulation induced by changes in surface water fluxes. *Nature* **351,** 729–732 (1991).
35. Manabe, S. & Stouffer, R. J. Coupled ocean-atmosphere model response to freshwater input: comparison to Younger Dryas event. *Paleoceanography* **12,** 321–336 (1997).
36. Fanning, A. F. & Weaver, A. J. Temporal-geographical meltwater influences on the North Atlantic Conveyor: Implications for the Younger Dryas. *Paleoceanography* **12,** 307–320 (1997).
37. Bond, G. C. *et al.* in *Mechanisms of Global Climate Change at Millennial Timescales* (eds Clark, P. U., Webb, R. S. & Keigwin, L. D.) 35–58 (Geophysical Monograph 112, American Geophysical Union, Washington DC, 1999).
38. Clark, P. U. *et al.* Freshwater forcing of abrupt climate change during the last glaciation. *Science* **293,** 283–287 (2001).
39. Fairbanks, R. G. A 17,000-year glacio-eustatic sea level record: influence of glacial melting rates on the Younger Dryas event and deep ocean circulation. *Nature* **342,** 637–642 (1989).
40. Clark, P. U., Mitrovica, J. X., Milne, G. A. & Tamisiea, M. Sea-level fingerprinting as a direct test for the source of global meltwater pulse 1A. *Science* (submitted).
41. Severinghaus, J. P., Sowers, T., Brook, E. J., Alley, R. B. & Bender, M. L. Timing of abrupt climate change at the end of the Younger Dryas interval from thermally fractionated gases in polar ice. *Nature* **391,** 141–146 (1998).
42. McManus, J. F., Oppo, D. W. & Cullen, J. L. A 0.5-million-year record of millennial-scale climate variability in the North Atlantic. *Science* **283,** 971–975 (1999).
43. Alley, R. B., Anandakrishnan, S. & Jung, P. Stochastic resonance in the North Atlantic. *Paleoceanography* **16,** 190–198 (2001).
44. Hostetler, S. W., Clark, P. U., Bartlein, P. J., Mix, A. C. & Pisias, N. Atmospheric transmission of North Atlantic Heinrich events. *J. Geophys. Res.* **104,** 3947–3952 (1999).
45. Hughen, K. A., Overpeck, J. T., Peterson, L. C. & Trumbore, S. Rapid climate changes in the tropical Atlantic region during the last deglaciation. *Nature* **380,** 51–54 (1996).
46. Peterson, L. C., Haug, G. H., Hughen, K. A. & Rohl, U. Rapid changes in the hydrologic cycle of the tropical Atlantic during the last glacial. *Science* **290,** 1947–1951 (2000).
47. Schulz, H., von Rad, U. & Erlenkeuser, H. Correlations between Arabian Sea and Greenland climate oscillations of the past 110,000 years. *Nature* **393,** 54–57 (1998).
48. Kienast, M., Steinke, S., Stattegger, K. & Calvert, S. E. Synchronous tropical South China Sea SST change and Greenland warming during deglaciation. *Science* **291,** 2132–2134 (2001).
49. Behl, R. J. & Kennett, J. P. Brief interstadial events in the Santa Barbara basin, NE Pacific, during the past 60 kyr. *Nature* **379,** 243–246 (1996).
50. Blunier, T. & Brook, E. J. Timing of millennial-scale climate change in Antarctica and Greenland during the last glacial period. *Science* **291,** 109–112 (2001).
51. Broecker, W. S. Paleocean circulation during the last deglaciation: A bipolar seesaw? *Paleoceanography* **13,** 119–121 (1998).
52. Crowley, T. J. North Atlantic deep water cools the southern hemisphere. *Paleoceanography* **7,** 489–497 (1992).
53. Schiller, A., Mikolajewicz, U. & Voss, R. The stability of the thermohaline circulation in a coupled ocean-atmosphere general circulation model. *Clim. Dyn.* **13,** 325–347 (1997).
54. Stocker, T. F. The seesaw effect. *Science* **282,** 61–62 (1998).
55. Oeschger, H. *et al.* in *Climate Processes and Climate Sensitivity* (eds Hansen, J. E. & Takahashi, T.) 299–306 (Geophysical Monograph 29, American Geophysical Union, Washington DC, 1984).
56. Mikolajewicz, U. & Maier-Reimer, E. Mixed boundary conditions in ocean general circulation models and their influence on the stability of the model's conveyor belt. *J. Geophys. Res.* **99,** 22633–22644 (1994).
57. Schmittner, A. & Weaver, A. J. Dependence of multiple climate states on ocean mixing parameters. *Geophys. Res. Lett.* **28,** 1027–1030 (2001).
58. Tziperman, E. Inherently unstable climate behaviour due to weak thermohaline ocean circulation. *Nature* **386,** 592–595 (1997).
59. Mikolajewicz, U., Maier-Reimer, E., Crowley, T. J. & Kim, K.-Y. Effect of Drake and Panamanian gateways on the circulation of an ocean model. *Paleoceanography* **8,** 409–426 (1993).
60. Ganopolski, A. & Rahmstorf, S. Rapid changes of glacial climate simulated in a coupled climate model. *Nature* **409,** 153–158 (2001).
61. Schmittner, A., Appenzeller, C. & Stocker, T. F. Enhanced Atlantic freshwater export during El Niño. *Geophys. Res. Lett.* **27,** 1163–1166 (2000).
62. Timmermann, A. *et al.* Increased El Niño frequency in a climate model forced by future greenhouse warming. *Nature* **398,** 694–696 (1999).
63. Johnsen, S. J. *et al.* Irregular glacial interstadials recorded in a new Greenland ice core. *Nature* **359,** 311–313 (1992).
64. Rind, D. *et al.* Effects of glacial meltwater in the GISS coupled atmosphere-ocean model: Part I: North Atlantic Deep Water response. *J. Geophys. Res.* **106,** 27335–27354 (2001).
65. Rahmstorf, S. & Ganopolski, A. Long-term global warming scenarios computed with an efficient coupled climate model. *Clim. Change* **43,** 353–367 (1999).
66. Mikolajewicz, U. & Voss, R. The role of the individual air-sea flux components in CO_2-induced changes of the ocean's circulation and climate. *Clim. Dyn.* **16,** 627–642 (2000).
67. Wood, R. A., Keen, A. B., Mitchell, J. F. B. & Gregory, J. M. Changing spatial structure of the thermohaline circulation in response to atmospheric CO_2 forcing in a climate model. *Nature* **399,** 572–575 (1999).
68. Joos, F., Plattner, G.-K., Stocker, T. F., Marchal, O. & Schmittner, A. Global warming and marine carbon cycle feedbacks on future atmospheric CO_2. *Science* **284,** 464–467 (1999).
69. Latif, M., Roeckner, E., Mikolajewicz, U. & Voss, R. Tropical stabilization of the thermohaline circulation in a greenhouse warming simulation. *J. Clim.* **13,** 1809–1813 (2000).
70. Delworth, T. L. & Dixon, K. W. Implications of the recent trend in the Arctic/North Atlantic Oscillation for the North Atlantic thermohaline circulation. *J. Clim.* **13,** 3721–3727 (2000).
71. Knutti, R. & Stocker, T. F. Limited predictability of the future thermohaline circulation close to an instability threshold. *J. Clim.* **15,** 179–186 (2002).
72. Stuiver, M. *et al.* INTCAL98 radiocarbon age calibration, 24,000 cal BP. *Radiocarbon* **40,** 1041–1083 (1998).
73. Kitigawa, H. & van der Plicht, J. Atmospheric radiocarbon calibration beyond 11,900 cal BP from Lake Suigetsu laminated sediments. *Radiocarbon* **42,** 369–380 (2000).
74. Bard, E., Arnold, M., Hamelin, B., Tisnerat-Laborde, N. & Cabioch, G. Radiocarbon calibration by means of mass spectrometric ^{230}Th/^{234}U and ^{14}C ages of corals: an updated database including samples from Barbados, Mururoa and Tahiti. *Radiocarbon* **40,** 1085–1092 (1998).
75. Cuffey, K. M. & Clow, G. D. Temperature, accumulation, and ice sheet elevation in central Greenland through the last deglacial transition. *J. Geophys. Res.* **102,** 26383–26396 (1997).
76. Grootes, P. M., Stuiver, M., White, J. W. C., Johnsen, S. J. & Jouzel, J. Comparison of oxygen isotope records from the GISP2 and GRIP Greenland ice cores. *Nature* **366,** 552–554 (1993).
77. Meese, D. A. *et al.* The Greenland Ice Sheet Project 2 depth-age scale: Methods and results. *J. Geophys. Res.* **102,** 26411–26423 (1997).
78. Rühlemann, C., Mulitza, S., Muller, P. J., Wefer, G. & Zahn, R. Warming of the tropical Atlantic Ocean and slowdown of thermohaline circulation during the last deglaciation. *Nature* **402,** 511–514 (1999).
79. Sachs, J. P., Anderson, R. F. & Lehman, S. J. Glacial surface temperatures of the southeast Atlantic Ocean. *Science* **293,** 2077–2079 (2001).
80. Steig, E. J. *et al.* Synchronous climate changes in Antarctica and the North Atlantic. *Science* **282,** 92–95 (1998).
81. Mulvaney, R. *et al.* The transition from the last glacial period in inland and near coastal Antarctica. *Geophys. Res. Lett.* **27,** 2673–2676 (2000).
82. Pisias, N. G., Mix, A. C. & Heusser, L. Millennial scale climate variability of the northeast Pacific Ocean and northwest North America based on radiolaria and pollen. *Quat. Sci. Rev.* **20,** 1561–1576 (2001).
83. Mix, A. C. *et al.* in *Mechanisms of Global Climate Change at Millennial Timescales* (eds Clark, P. U., Webb, R. S. & Keigwin, L. D.) 127–148 (Geophysical Monograph 112, American Geophysical Union, Washington DC, 1999).
84. Thompson, L. G. *et al.* Late glacial stage and Holocene tropical ice core records from Huascaran, Peru. *Science* **269,** 46–50 (1995).
85. Thompson, L. G. *et al.* A 25,000-year tropical climate history from Bolivian ice cores. *Science* **282,** 1858–1864 (1998).
86. Bard, E., Rostek, F. & Sonzogni, C. Interhemispheric synchrony of the last deglaciation inferred from alkenone paleothermometry. *Nature* **385,** 707–710 (1997).
87. Little, M. G. *et al.* Trade wind forcing of upwelling seasonality, and Heinrich events as a response to sub-Milankovitch climate variability. *Paleoceanography* **12,** 568–576 (1997).
88. Charles, C. D., Lynch-Stieglitz, J., Ninnemann, U. S. & Fairbanks, R. G. Climate connections between the hemispheres revealed by deep sea sediment core/ice core correlations. *Earth Planet. Sci. Lett.* **142,** 19–27 (1996).
89. Petit, J. R. *et al.* Climate and atmospheric history of the past 420,000 years from the Vostok ice core, Antarctica. *Nature* **399,** 429–436 (1999).
90. Jouzel, J. *et al.* A new 27 ky high resolution East Antarctic climate record. *Geophys. Res. Lett.* **28,** 3199–3202 (2001).

Acknowledgements

We thank G. Bond, J. Jouzel, A. Mix, R. Muscheler, J. Sachs and J. van der Plicht for providing data, the NOAA-NGDC Paleoclimate Program for their data repository, and S. Hostetler, A. Mix, A. Schmittner and R. Stouffer for comments. This work was supported by grants from the Earth System History Program of the US NSF (P.U.C. and N.G.P.), the Swiss NSF (T.F.S.) and the Canadian NSERC (A.J.W.).

Correspondence and requests for materials should be addressed to P.U.C. (e-mail: clarkp@ucs.orst.edu).